



ORIGINAL PAPER

DECADAL CYCLES OF EARTH ROTATION, MEAN SEA LEVEL AND CLIMATE, EXCITED BY SOLAR ACTIVITYYavor CHAPANOV^{1)*}, Cyril RON²⁾ and Jan VONDRÁK²⁾

1) National Institute of Geophysics, Geodesy and Geography, Bulgarian Academy of Sciences,
Acad. G. Bonchev Str. Bl.3, Sofia 1113, Bulgaria

2) Astronomical Institute, Czech Academy of Sciences, Boční II 1401, 141 00 Prague 4, Czech Republic

*Corresponding author's e-mail: yavor.chapanov@gmail.com

ARTICLE INFO**Article history:**

Received 15 January 2017

Accepted 3 March 2017

Available online 23 March 2017

Keywords:

Earth rotation
Solar activity
Mean sea level
Climate
ENSO
Decadal cycles

ABSTRACT

The solar activity affects all surface geosystems, including weather and climate indices, winds, rains, snow covers, mean sea level, river streamflows and other hydrological cycles. The mean sea level and polar ice changes cause common variations of the principal moments of inertia and Earth rotation with decadal, centennial and millennial periods. The mean sea level, Earth rotation and climate indices have also some oscillations with periods below 40 years, whose origin is not connected with the known tidal and solar effects. The shape of solar cycles is rather different from sinusoidal form, so they affect geosystems by many short-term harmonics. A possible solar origin of decadal variations of Earth rotation, mean sea level and climate indices is investigated by the harmonics of Jose, de Vries and Suess cycles with centennial periods of 178.7, 208 and 231 years. The common decadal cycles of solar-terrestrial influences are investigated by long time series of Length of Day (LOD), Mean Sea Level (MSL) variations at Stockholm, El-Niño/Southern Oscillation (ENSO), temperature and precipitation over Eastern Europe, Total Solar Irradiance (TSI), Wolf's Numbers W_n and North-South solar asymmetry. A good agreement exists between the decadal cycles of LOD, MSL, climate and solar indices whose periods are between 12-13, 14-16, 16-18 and 28-33 years. The new linear models of the decadal common Earth and solar cycles may help for long term forecasts of many global and local changes.

1. INTRODUCTION

The investigation of the variations of Earth parameters in time and their connection with solar activity is very important in studying the natural risks and the environmental changes. The new complex local and global models of solar-terrestrial interconnections may improve long term forecasts of danger climate events like severe dry or wet, floods, extremely high or low temperatures.

The existing long climatic and astronomical time series with centennial time spans are useful to study common decadal and centennial cycles of the solar activity, climate, Earth rotation and other terrestrial phenomena. The bicentennial solar cycles consist of several known oscillations. Jose (1965) points out a repeating solar system configuration of the 4 outer planets with period of 178.7 years. He suggests this configuration modulates the solar cycles. Sharp (2010) suggests another value - 171.44 years, which is the synodic period of Uranus and Neptune. Some authors study solar periodicity 205-210 years (de Vries cycle) and 230 years (Suess cycle) and they consider the bicentennial solar cycles as one of the most intensive solar cycles. The variation of

cosmogenic isotopes ^{14}C and ^{10}Be concentration in terrestrial archives is the main instrument to study solar activity cycles in the past. Vasilev et al. (1999) and Muscheler et al. (2003) determine that the 200 year solar activity cycle (de Vries cycle) is a dominant cycle during the Holocene by means of tree rings radiocarbon. Eddy (1976) considers the grand solar minima as manifestations of the de Vries cycle during the past millennia. Wagner et al. (2001) study the bicentennial periodicity by ^{10}Be concentration in Greenland ice as a proxy for solar activity variations 25Kyr-50Kyr before present (BP). Sonett and Suess (1984) show correlation between the bicentennial cycles of the isotope ^{14}C concentration and the radial growth of tree rings from eastern California. Schimmelmann et al. (2003) demonstrate the connection between the bicentennial solar cycles and some climatic parameters. Haeberli and Holzhauser (2003) point out the climate response to the grand solar minima based on Alpine glaciers data. Wiles et al. (2004) make similar conclusion about glacier expansion in Alaska. The bicentennial climatic periodicities are detected in Europe, North and South America, Asia, Tasmania, Antarctica and Arctic, and

in the ocean sediments (Sonett and Suess, 1984; Peterson et al., 1991; Anderson, 1992, 1993; Cook et al., 1996; Zolitschka, 1996; Dean, 1997; Cini Castagnoli et al., 1998; Qin et al., 1999; Hong et al., 2000; Hodell et al., 2001; Nyberg et al., 2001; Roig et al., 2001; Yang et al., 2002; Fleitman et al., 2003; Haeberli and Holzhauser, 2003; Hu et al., 2003; Schimmelmann et al., 2003; Soon and Yaskell, 2003; Prasad et al., 2004; Raspopov et al., 2004; Wiles et al., 2004; Wang et al., 2005). The bicentennial climatic signals should reveal significant global effects. These effects are synchronous bicentennial oscillations of the mean sea level and polar ice thickness, due to global water redistribution between ocean and continental polar ice. The polar ice thickness increases and the mean sea level decreases during the bicentennial cold events, followed by the decrease of the mean Earth radius and the principal moment of inertia relative to the rotational axis. Any change of the principal moment of inertia leads to significant variations of the Earth rotation, due to the conservation of the Earth angular momentum.

Ron et al. (2012) determine new values for the periods of de Vries cycle – 208 years and 231 years - for Suess cycle. These values are obtained by analysis of Total Solar Irradiance (TSI), Mean Sea Level (MSL) and Universal Time data and they will be used in this work to determine proper values of common solar and terrestrial decadal cycles.

The solar activity affects terrestrial systems by means of direct radiation over Earth surface, charged particles of the solar wind, and the solar magnetic field. The solar wind directly affects Earth magnetic field, ionosphere and atmosphere. The variations of solar magnetic field modulate solar wind and cosmic rays in the frame of the solar system. The cosmic rays near Earth are modulated by Earth magnetic field variations, too. In the past, it was supposed that the increase of cosmic rays may strongly affect the climate by intensifying cloud formation, following by significant cooling events. After some debates, it was clear that the influence of cosmic rays on clouds is not so strong. But recently, another mechanism of climate variations, due to cosmic rays was proposed (Kilifarska and Haight, 2005; Kilifarska, 2008, 2011; Velinov et al., 2005). According to the new models, the cosmic rays produce a ionization of the atmosphere, changes of atmosphere conductivity, lightning, and an increase of ozone concentration. The ozone plays significant role in climate variations, so the new models of cosmic ray influences on Earth atmosphere may explain the observed correlation between cosmic rays and climate variations.

The solar activity variations are presented by several numerical indices. The most popular of them are indices of sunspots, Wolf's numbers and TSI. The sunspots and Wolf's numbers are observed during the last 4 centuries, while the real observations of TSI are available for the last decades. The solar data (sunspots and TSI) for the past periods are reconstructed over

millennial time scale (Steinhilber et al., 2009; Solanki et al., 2004; Bard et al., 2001) and these data are used in Ron et al. (2012) to determine the parameters of common bicentennial solar-terrestrial cycles. These reconstructions are rather thin with step size 5 or 10 years, so the decadal TSI oscillations are determined in this research by more dense TSI annual reconstruction (Lean, 2000).

The Wolf's numbers represent the variations of solar wind and TSI. It is possible to calculate a new index of North-South (N-S) solar asymmetry, based on sunspot numbers over the North and South solar hemisphere. The N-S solar asymmetry represents variations of the solar magnetic field. The time series of TSI, Wolf's numbers and N-S solar asymmetry have different spectra, so their influences on terrestrial cycles may vary in frequency, amplitude and phase.

2. LONG TIME SERIES

The common decadal cycles of solar-terrestrial influences are investigated by long time series of Length of Day (LOD), MSL variations at Stockholm, El-Niño/Southern Oscillation (ENSO), temperature and precipitation over Eastern Europe, TSI, Wolf's Numbers (W_n) and N-S solar asymmetry (Fig. 1).

The daily values of W_n for the period 1818.0-now are provided by the Royal Observatory of Belgium (Fig. 1, A). The time series of the TSI for the period 1610.5-2000.5 (Fig. 1, B) are reconstructed by Lean (2000). The Earth rotation data for the period 1623.5-2005.5 (Fig. 1, F) are available from the IERS EOP Data Center. The detrended values of the MSL at Stockholm (Ekman, 2003) are shown in Figure 1, E. The annual time series of LOD are combination between the solution of Stephenson and Morrison (1984), based on lunar eclipses and star occultations before 1955 and modern determinations afterwards. Another more dense time series is the solution C02 of IERS 1830-now (Fig. 1, F). The precipitation and temperature over part of Eastern Europe for the period 1767-2000 are determined from the gridded data (Casty et al., 2005, 2007) covered the trapezoid, shown in Figure 1, (I). Casty et al. (2005, 2007) reconstructed European monthly temperature and precipitation for the 500 hPa geopotential, covering the last 235 years by means of a database of monthly climate observations since 1900 (Mitchell and Jones, 2005) and the NCEP-NCAR reanalysis of the data since 1948 (Kalnay et al., 1996; Kistler et al., 2001). The European gridded monthly temperature and precipitation data cover area from 80°-30°N and 50°W-40°E on a 0.5° grid. The climatic data of part of Eastern Europe between 11°-30°E and 41°-51°N (Fig. 1, I) are determined from 710 grids (0.5°×0.5°) over the ground. The monthly temperature (Fig. 1, D) and precipitation (Fig. 1, C) are determined from their gridded values by Danish Method average. The Danish Method (Kubik, 1982; Juhl, 1984; Kegel, 1987) provides robust estimation of mean values and eliminates all data outliers. The index S_a of the N-S

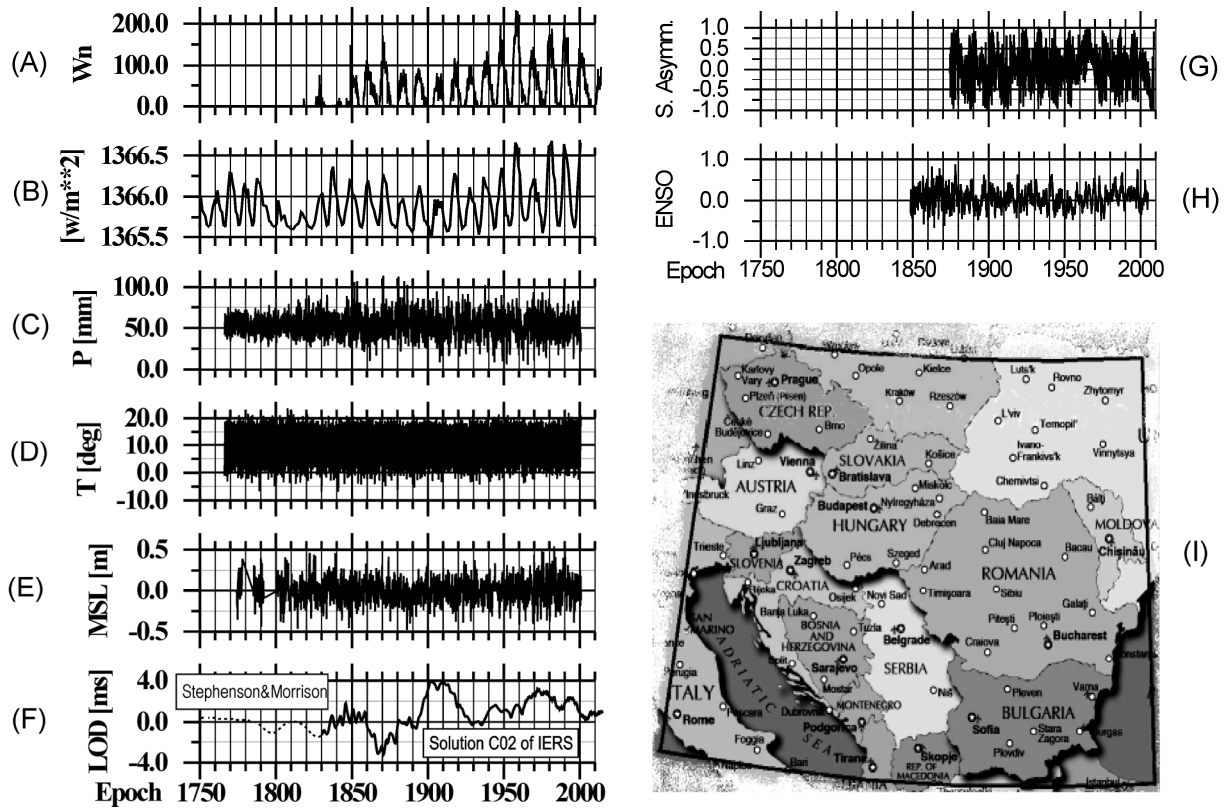


Fig. 1 Long time series of solar and terrestrial data: W_n (A); TSI (B); precipitation (C) and temperature (D) over part of Eastern Europe (I); MSL at Stockholm (E); LOD (F); Index of N-S solar asymmetry (G) and ENSO (H). The LOD time series is composed by the solution of Stephenson and Morrison (1984) before 1830 (dotted line) and by the solution C02 of IERS after (solid line).

solar asymmetry since 1874.4 (Fig. 1, G) is calculated from the sunspot numbers of the North solar hemisphere S_n and South solar hemisphere S_s by the expression $S_a = (S_s - S_n) / (S_s + S_n)$. The index of ENSO is used for the period 1848.5-2005.0 (Fig. 1, H).

3. METHOD OF PARTIAL FOURIER APPROXIMATION

The periodical variations are derived from the data by means of partial Fourier approximation based on the Least-Squares (LS) estimation of Fourier coefficients (Chapanov et al., 2015; Ron et al., 2012). The Partial Fourier approximation $F(t)$ of discrete data is given by

$$F(t) = f_0 + f_1(t - t_0) + \sum_{k=1}^n a_k \sin k \frac{2\pi}{t_E - t_B} (t - t_0) + b_k \cos k \frac{2\pi}{t_E - t_B} (t - t_0), \quad (1)$$

where t_0 , t_B and t_E are the mean, first and last epochs of observations, respectively, f_0 , f_1 , a_k and b_k are unknown coefficients and n is the number of harmonics of the partial sum, which covers all oscillations with periods between $(t_E - t_B)/n$ and $(t_E - t_B)$.

The application of the LS estimation of Fourier coefficients needs at least $2n+2$ observations, so the number of harmonics n is chosen significantly smaller than the number N of sampled data f_i . The small number of harmonics n yields to LS estimation of the coefficient errors, too. The period of the first long-periodical harmonic in (1) depends on the observational time span in case of classic Fourier approximation, but here it is possible to decrease the value of the first harmonic, so the estimated frequencies may cover the desired set of real oscillations. This method allows a flexible and easy separation of harmonic oscillations into different frequency bands by the formula

$$B(t) = \sum_{k=m_1}^{m_2} a_k \sin k \frac{2\pi}{t_E - t_B} (t - t_0) + b_k \cos k \frac{2\pi}{t_E - t_B} (t - t_0), \quad (2)$$

where the desired frequencies $\omega_k = k \frac{2\pi}{t_E - t_B}$ are

limited by the bandwidth

$$\frac{2\pi m_1}{t_E - t_B} \leq \omega_k \leq \frac{2\pi m_2}{t_E - t_B} \quad (3)$$

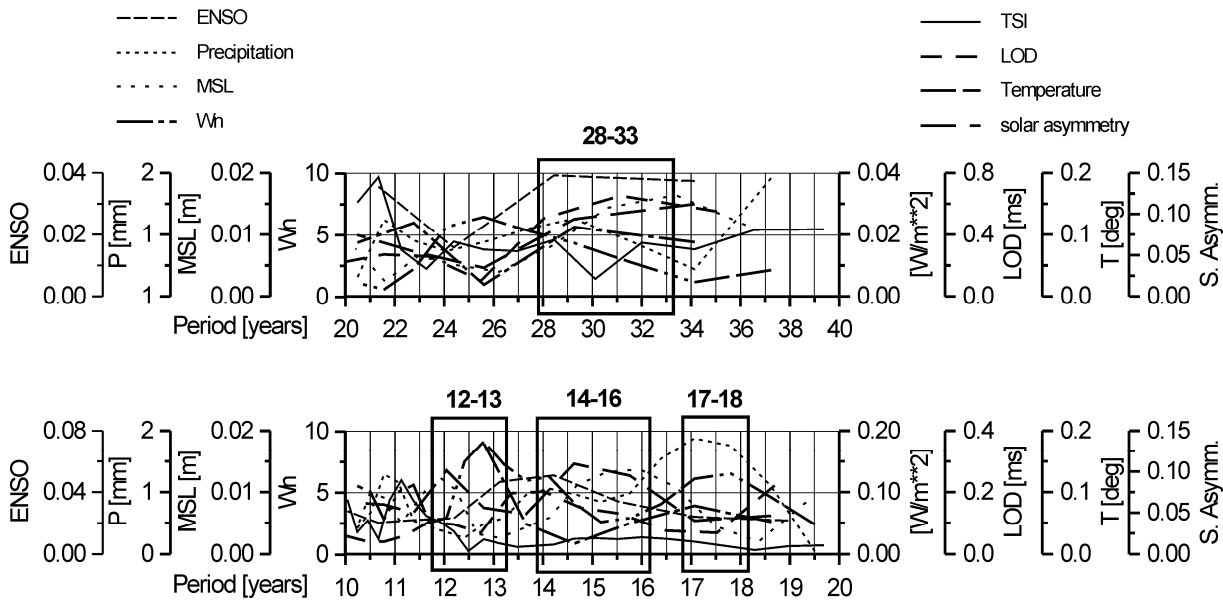


Fig. 2 Spectra of ENSO, precipitation and temperature over part of Eastern Europe, MSL at Stockholm, W_n , TSI, LOD and Index of N-S solar asymmetry.

After estimating the Fourier coefficients, it is possible to identify a narrow frequency zone presenting significant amplitude, and defining a given cycle. Then this cycle can be reconstructed in time domain as the partial sum limited to the corresponding frequency bandwidth. Doing this for terrestrial and solar time series, we shall identify their respective cycles, isolate and compare the common ones.

4. SPECTRAL ANALYSES

The amplitude spectra of chosen time series are calculated by means of the Fast Fourier Transform Method. The decadal spectral peaks outside the known 11-year Schwabe and 22-year Hale solar cycles and 18.6-year period of Lunar node are shown in Figure 2.

The decadal oscillations below 35 years of Earth and solar data have several bands with close spectral peaks and we may choose 4 of them with most remarkable local maxima: 12-13 years; 14-16 years; 17-18 years and 28-33 years. The boundaries of these bands are not strictly determined, because the periods of common solar-terrestrial cycles may be close to them or lie inside the bands.

5. COMMON SOLAR AND EARTH CYCLES

The common solar and Earth cycles are derived by the Method of Partial Fourier Approximation. The oscillations of these cycles are determined by superposition of 2 or more neighbor harmonics, whose periods are close to or lie inside the chosen band.

5.1. PERIODS 12-13 YEARS

The cycles with periods from band 12-13 years of pairs MSL- W_n ; P-LOD; and ENSO- N-S solar

asymmetry are compared in Figure 3. The used MSL data are for the period 1801.1-2000.9. The MSL oscillations are calculated as superposition of 15-th and 16-th harmonics (with periods 13.3 and 12.5 years) of approximation (2). The Wolf's numbers variations from this band are calculated by approximation (2) with superposition of 15-th and 16-th harmonics with periods 13.0 and 12.2 years. The comparison of MSL and W_n cycles shows relatively good agreement for the time intervals 1820-1890 and 1940-2000 with time lag of about 3 years whereas variations for the time interval 1890-1940 are out of phase.

Much better is the comparison of LOD and precipitation cycles. The LOD oscillations are calculated by 14-th and 15-th harmonics with periods 13.2 and 12.3 years. The precipitation cycles are calculated by 18-th and 19-th harmonics with periods 13.0 and 12.3 years. The amplitude variations of both time series are almost identical with very small phase deviations. The time lag is about 4 years. The correlation coefficient is negative, so this is not direct effect of continental climate on Earth rotation, but it represents the corresponding MSL variations due to water evaporation, followed by water mass transport over the Eastern Europe.

The ENSO oscillations are determined by the 12th and 13th harmonics of its Partial Fourier Approximations, whose periods are 12.0 and 13.0 years. The N-S solar asymmetry oscillations are determined by the 9th and 10th harmonics with periods 13.9 and 12.5 years. The variations of amplitude of both time series are almost identical. Phase reverse occurs around 1950 together with a jump of time lag, which value is less than 2 years between the time series.

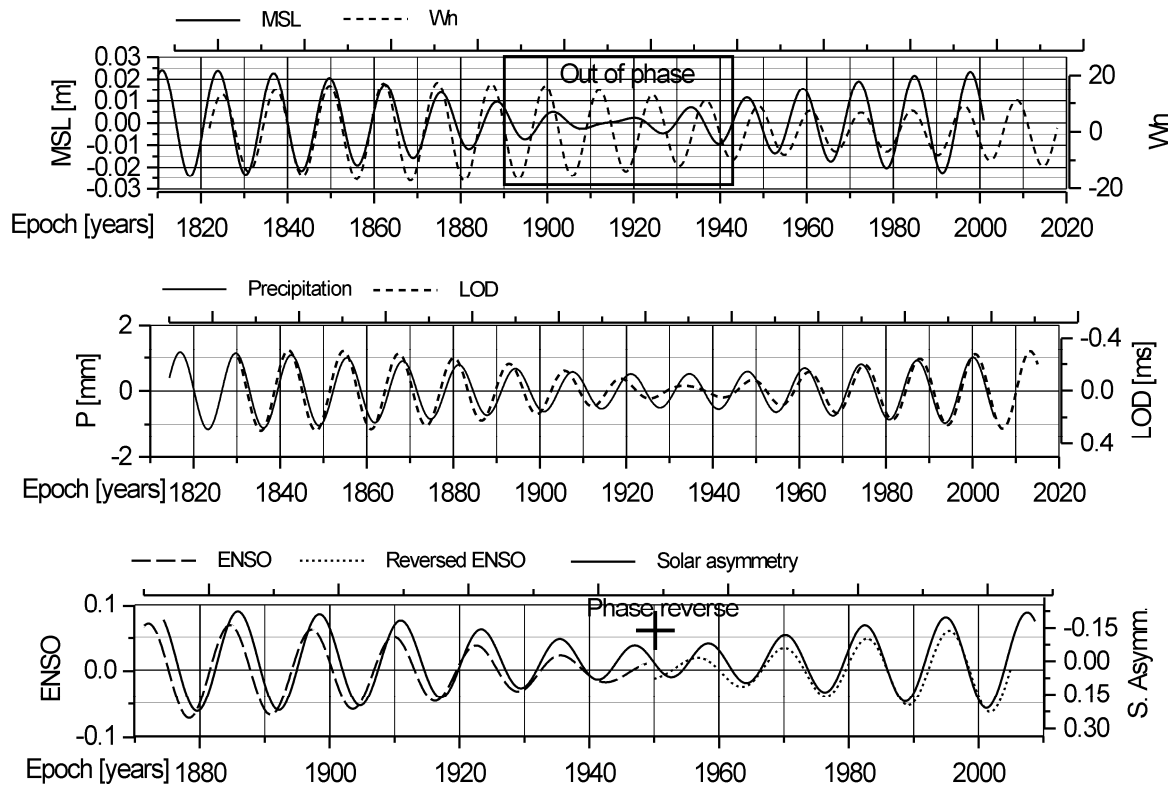


Fig. 3 Common cycles with periods 12-13 years of pairs MSL- W_n ; P-LOD; and ENSO- N-S solar asymmetry.

5.2. PERIODS 14-16 YEARS

The cycles with periods from band 14-16 years of pairs MSL-LOD; P- W_n ; and ENSO- N-S solar asymmetry are compared in Figure 4. The MSL cycles are calculated by 13th and 14th harmonics with periods 15.4 and 14.3 years. The LOD oscillations are calculated by 12th and 13th harmonics with periods 15.4 and 14.2 years. The precipitation cycles are calculated by 15th, 16th and 17th harmonics with periods 15.6 14.7 and 13.8 years. The W_n cycles are calculated by 12th, 13th and 14th harmonics with periods 16.4, 15.0 and 14.0 years. The ENSO oscillations are determined by the 10th and 11th harmonics with periods 15.6 and 14.2 years. The N-S solar asymmetry oscillations are determined by the 8th and 9th harmonics with periods 15.6 and 13.9 years.

A relatively good agreement occurs between the variations of the phase and amplitude of MSL and LOD oscillations. A partial correlation appears between the variations of Wolf's numbers and Eastern Europe precipitation, where good agreement exists for the time intervals 1870-1920 and 1950-2000. These cycles are out of phase for the time intervals 1820-1870 and 1920-1950. The ENSO cycles are strongly affected by the variations of N-S solar asymmetry – the amplitude and phase variations are almost synchronous with phase reverse in 1970.

5.3. PERIODS 16-18 YEARS

The cycles with periods from band 16-18 years of pairs LOD-TSI; MSL-P; and ENSO- N-S solar asymmetry are compared in Figure 5. The LOD oscillations are calculated by 10th and 11th harmonics with periods 18.4 and 16.8 years. The TSI cycles are calculated by harmonics 21-24 whose periods are between 16.2, and 18.5 years. The MSL cycles are calculated by 11th and 12th harmonics with periods 18.1 and 16.6 years. The precipitation cycles are calculated by 13th and 14th harmonics with periods 18.0 and 16.7 years. The ENSO oscillations are determined by the 9th and 10th harmonics with periods 17.4 and 15.6 years. The N-S solar asymmetry oscillations are determined by the 7th and 8th harmonics with periods 17.8 and 15.6 years.

A relatively good agreement occurs between the LOD and TSI variations of the amplitudes. The phase reverses during a short time interval 1900-1935. The oscillations of pairs MSL-P and ENSO- N-S solar asymmetry have good agreement with small amplitude deviation between ENSO and solar asymmetry.

5.4. PERIODS 28-33 YEARS

The cycles with periods from band 28-33 years of time series MSL- W_n ; P-LOD-TSI; and ENSO- N-S solar asymmetry are compared in Figure 6. The MSL

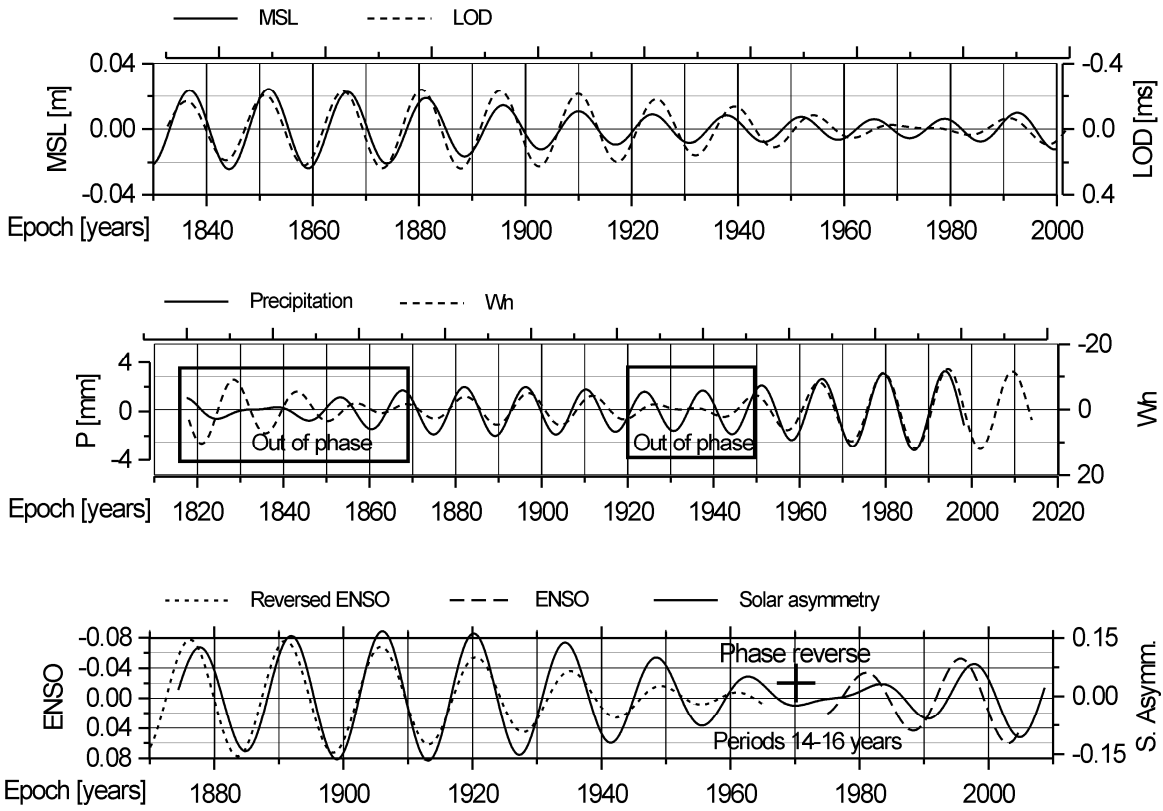


Fig. 4 Common cycles with periods 14-16 years of pairs MSL-LOD; P- W_h ; and ENSO- N-S solar asymmetry.

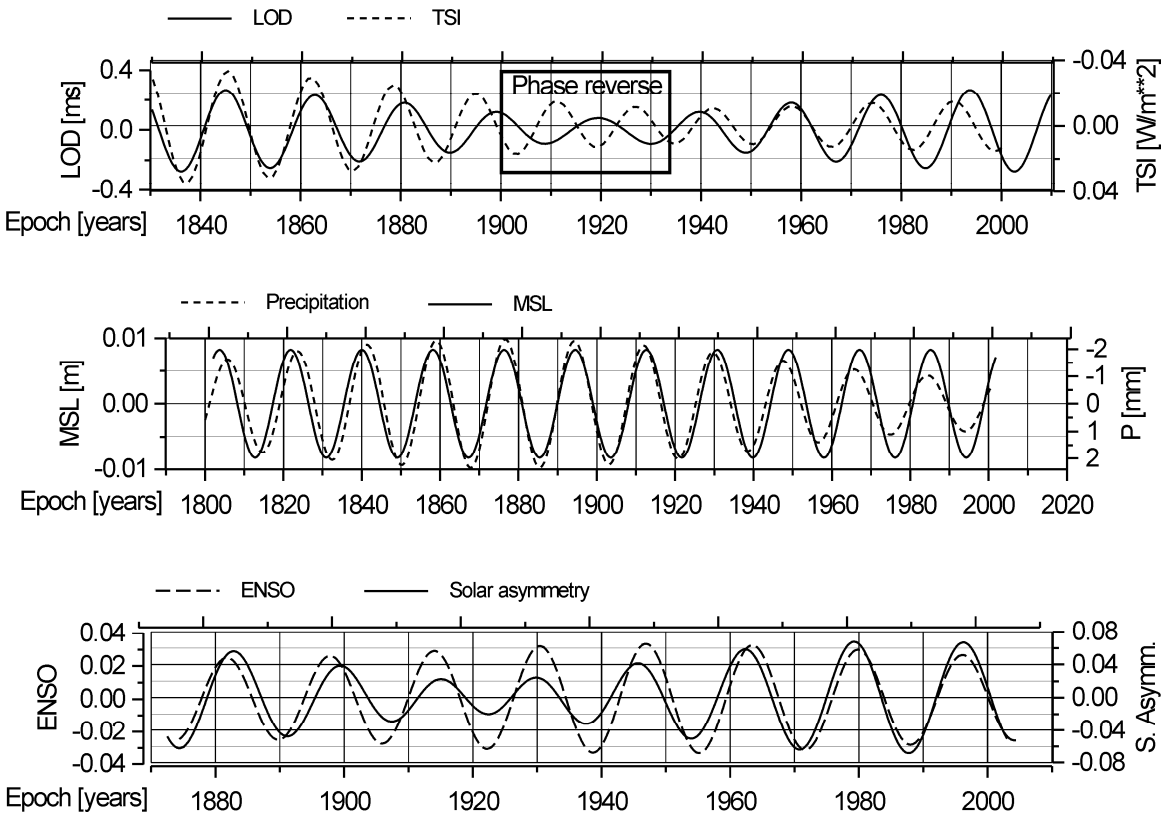


Fig. 5 Common cycles with periods 17-18 years of pairs LOD-TSI; MSL-P; and periods 16-18 years of pair ENSO- N-S solar asymmetry.

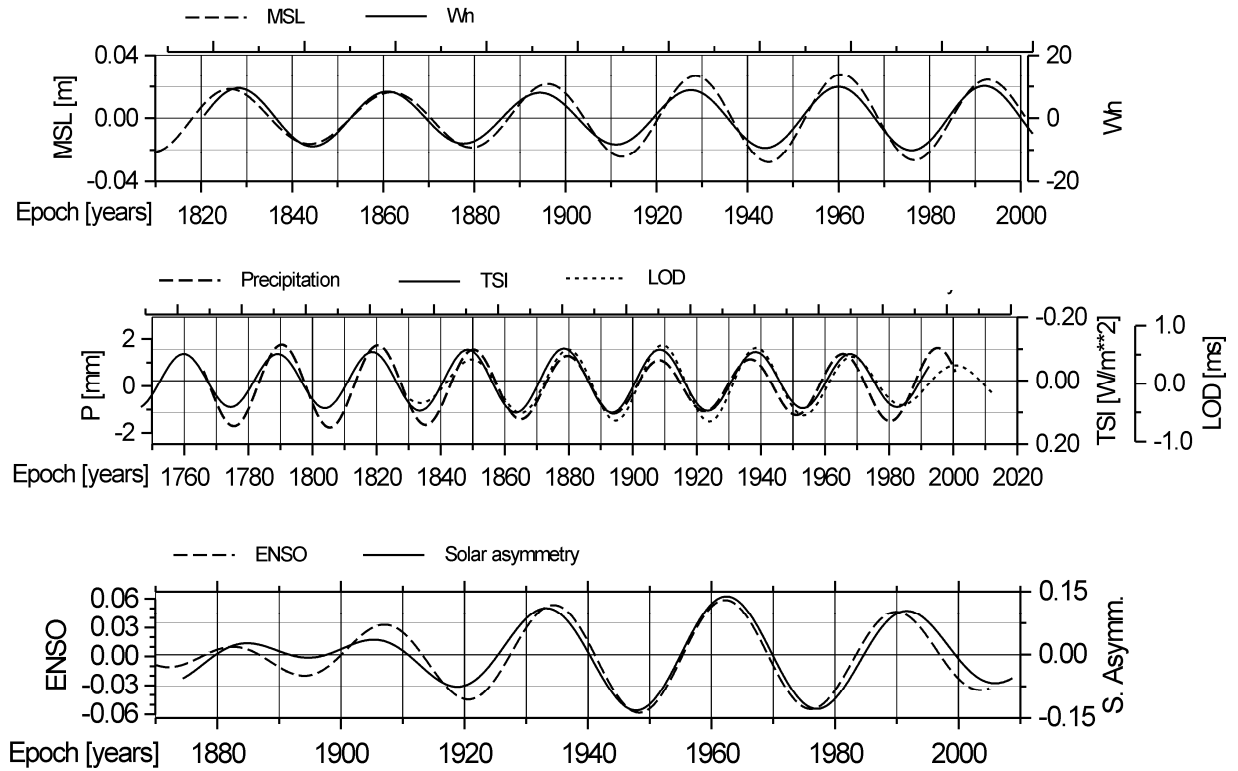


Fig. 6 Common cycles with periods 25-33 years of time series MSL- W_n ; P- LOD-TSI; and ENSO- N-S solar asymmetry.

cycles are calculated by the 6th and 7th harmonics with periods 33.3 and 28.5 years. The W_n cycles are calculated by the 6th and 7th harmonics with periods 32.7 and 28.0 years. The precipitation cycles are calculated by 7th and 8th harmonics with periods 33.5 and 29.3 years. The TSI cycles are calculated by 12th, and 13th harmonics with periods 32.3, and 29.8 years. The LOD oscillations are calculated by 6th and 7th harmonics with periods 30.7 and 26.3 years. The ENSO oscillations are determined by the 5th and 6th harmonics with periods 31.3 and 26.0 years. The N-S solar asymmetry oscillations are determined by the 4th and 5th harmonics with periods 31.2 and 25.0 years. Nevertheless the choice of different individual frequencies of these cycles, the presented curves in Figure 6 expose excellent agreement both in amplitude and phase. This means that inside the chosen frequency bands exists some powerful oscillator that forces the observed cycles.

6. HARMONICS OF JOSE, DE VRIES AND SUESS CYCLES

6.1. MODELS OF JOSE, DE VRIES AND SUESS CYCLES

The models of Jose, de Vries and Suess cycles based on Partial Fourier approximation of Earth and solar data are

$$F_i(t) = f_{i,0} + f_{i,1}(t-t_0) + \sum_{k=1}^n a_{i,k} \sin k \frac{2\pi}{P_i}(t-t_0) + b_{i,k} \cos k \frac{2\pi}{P_i}(t-t_0) \quad (4)$$

$i = 1, 2, 3$

where t_0 is the mean epoch of observations, $f_{i,0}$ and $f_{i,1}$ are linear coefficients, $a_{i,k}$ and $b_{i,k}$ are harmonic coefficients and n is the number of harmonics of the partial sum. The periods P_i correspond to the Jose, de Vries and Suess cycles:

$$\begin{aligned} P_1 &= 178.7 \text{ years (Jose cycle);} \\ P_2 &= 208.0 \text{ years (de Vries cycle);} \\ P_3 &= 231.0 \text{ years (Suess cycle).} \end{aligned} \quad (5)$$

The models (4) are applied to time series of climatic, LOD (according to the solution of Stephenson and Morrison, 1984), MSL and TSI data, whose time span is greater than 231 years. The phases $\Phi_{i,k} = \text{atan}(b_{i,k}/a_{i,k})$ of each harmonic of models (4) of P, LOD, MSL and TSI data are compared and analyzed in the next section.

6.2. DECADAL HARMONICS OF JOSE, DE VRIES AND SUESS CYCLES

The decadal oscillations of P, LOD, MSL and TSI, corresponding to the harmonics of Jose, de Vries and Suess cycles are determined by models (4) and (5). The Tables 1, 2 and 3 include harmonics with

Table 1 Harmonics of 178.7-year Jose cycle with periods below 30 years.

Harmonics number	Period [years]	Time series pair	Phase difference [degree]
6	29.8	LOD – MSL	5.3
		TSI – LOD	19.4
		TSI – P	32.9
8	22.3	LOD – MSL	6.6
		TSI – LOD	0.3
		TSI – P	5.9
9	19.9	TSI – P	12.3
10	17.9	LOD – MSL	3.4
		TSI – LOD	16.3
		TSI – P	7.9
11	16.2	TSI – MSL	2.6
14	12.8	LOD – MSL	2.0
		TSI – LOD	7.6
23	7.8	LOD – MSL	2.0
		TSI – LOD	11.9
		TSI – P	23.7

Table 3 Harmonics of 231-year Suess cycle with periods below 33 years.

Harmonics number	Period [years]	Time series pair	Phase difference [degree]
7	33.0	TSI – MSL	2.1
8	28.9	LOD – MSL	0,6
		TSI – LOD	28.6
		TSI – P	31.0
9	25.7	TSI – LOD	4.1
15	15.4	LOD – MSL	5.2
		TSI – LOD	4.1
		TSI – P	0.1
16	14.4	LOD – MSL	5.3
		TSI – P	17.6
26	8.9	LOD – MSL	8.1
34	6.8	LOD – MSL	7.8
		TSI – LOD	34.9
		TSI – P	18.2

periods below 33 years for data pairs with small phase differences. All presented harmonics point out to pairs of time series with small phase difference. We may consider a given harmonic as dominating over terrestrial events, if at least two pairs of time series are with very small phase differences – less than 10 degrees.

The harmonics with phase differences less than 10 degrees are:

Table 2 Harmonics of 208-year de Vries cycle with periods below 30 years.

Harmonics number	Period [years]	Time series pair	Phase difference [degree]
7	29.7	LOD – MSL	8.0
		TSI – LOD	9.6
		TSI – P	15.2
9	23.1	TSI – P	5.4
10	20.8	TSI – P	15.8
12	17.3	LOD – MSL	6.3
		TSI – LOD	26.2
		TSI – P	30.9
18	11.6	LOD – MSL	0.4
		TSI – LOD	4.9
		TSI – P	21.3
22	9.5	LOD – MSL	7.5
		TSI – LOD	32.0
		TSI – P	15.4
27	7.7	LOD – MSL	6.7
		TSI – LOD	9.9
		TSI – P	3.0

- Jose cycle: 22.3yr; 17.9yr; 16.2yr; 12.8yr; 7.8yr;
- De Vries cycle: 29.7yr; 23.1yr; 11.6yr; 7.7yr;
- Suess cycle: 33.0yr; 25.7yr; 15.4yr; 8.9yr; 6.8yr.

Next perspective study of decadal solar-terrestrial oscillations may concern oscillations with the following periods: 33.0; 29.7yr; 28.9yr; 25.7yr; 23.1yr; 22.3yr; 17.9yr; 17.3yr; 16.2yr; 15.4yr; 14.4yr; 12.8yr; and 11.6yr. The oscillations with subdecadal periods, like 9.5yr, 8.9yr, 7.8yr, 7.7yr, and 6.8yr are perspective in study the dependence of ENSO variations and solar cycles.

7. CONCLUSIONS

The shapes of decadal and centennial solar cycles are rather different from sinusoidal form, and this is the reason to generate a lot of subdecadal and decadal harmonics. These harmonics are visible as common cycles with periods 1-9, 12-19 and 23-33 years in various time series of Earth phenomena like Earth rotation, mean sea level, climate, etc. The Total Solar Irradiance (TSI), Wolf's Numbers (W_n) and North-South (N-S) solar asymmetry expose different spectral peaks, amplitude modulation and phases from these bands. These solar time series represent thermal heating over the Earth, solar wind (space weather) and solar magnetic field variations. The decadal cycles of N-S solar asymmetry strongly affect corresponding cycles of El Nino/Southern Oscillation (ENSO). The decadal oscillations of LOD and precipitation over the continents are affected by

the TSI variations, while the MSL oscillations – mainly by the Wolf's numbers. The LOD, MSL and precipitation cycles with periods below 20 years are affected by the harmonics of Wolf's numbers. The common cycles with periods 26-33 years of time series MSL- W_n ; P- LOD-TSI; and ENSO- N-S solar asymmetry have excellent agreement of amplitude and phase modulation. The common cycles with periods 17-18 years of pairs LOD-TSI; MSL-P; and periods 16-18 years of pair ENSO- N-S solar asymmetry have good agreement with small amplitude deviations and phase reverse. The common cycles with periods 14-16 years of pairs MSL-LOD; P- W_n ; and ENSO- N-S solar asymmetry have good agreement with phase reverse of ENSO event and some parts out of phase in case of precipitation. The common cycles with periods 12-13 years of pairs MSL- W_n ; P-LOD; and ENSO- N-S solar asymmetry have good agreement with phase reverse of ENSO event and a short part out of phase in case of MSL.

The decadal harmonics of TSI, LOD, MSL, precipitation and temperature over the Eastern Europe are calculated by models of Jose, de Vries and Suess cycles with periods of 178.7, 208 and 231 years and their phase differences are compared. This comparison yields several perspective decadal cycles with periods 33.0; 29.7yr; 28.9yr; 25.7yr; 23.1yr; 22.3yr; 17.9yr; 17.3yr; 16.2yr; 15.4yr; 14.4yr; 12.8yr; and 11.6yr to study the significant solar-terrestrial influences and to create new adequate linear models.

ACKNOWLEDGEMENTS

We thank to the anonymous referees for important comments and suggestions on the manuscript. This research was financially supported by the grant No. 13-15943S awarded by the Grant Agency of the Czech Republic .

REFERENCES

- Anderson, R.Y.: 1992, Possible connection between surface wind, solar activity and the Earth's magnetic field. *Nature*, 358, 6381, 51–53. DOI: 10.1038/358051a0
- Anderson, R.Y.: 1993, The varve chronometer in Elk Lake record of climatic variability and evidence for solar-geomagnetic-14C-climate connection. In: Bradbury, J.P., Dean, W.E. (Eds.), *Elk Lake, Minnesota: Evidence for rapid climate change in the North-Central United States*. Geological Society of America, Special Paper, 276, 45–68. DOI: 10.1130/SPE276-p45
- Bard, E., Raisbeck, G., Yiou, F. and Jouzel, J.: 2000, Solar irradiance during the last 1200 years based on cosmogenic nuclides. *TELLUS B*, 52, 3, 985–992. DOI: 10.1073/pnas.0605064103
- Casty, C., Handorf, D. and Sempf, M.: 2005, Combined climate winter regimes over the North Atlantic/European sector 1766–2000. *Geophysical Research Letters*, 32, 13. DOI: 10.1029/2005GL022431
- Casty, C., Raible, C.C., Stocker, T.F., Luterbacher, J. and Wanner, H.: 2007, A European pattern climatology 1766–2000. *Climate Dynamics*, 29, 7, 791–805. DOI: 10.1007/s00382-007-0257-6
- Chapanov, Ya., Ron, C. and Vondrák, J.: 2015, Millennial cycles of mean sea level excited by Earth's orbital variations. *Acta Geodyn.Geomater.*, 12, 3 (179), 259–266. DOI: 10.13168/AGG.2015.0028
- Cini Castagnoli, G., Bonino, G., Della Monica, P., Procopio, S. and Taricco, C.: 1998, On the solar origin of the 200y Suess wiggles: Evidence from thermoluminescence in sea sediments. *Il Nuovo Cimento*, 21C, 2, 237–241.
- Cook, E.R., Buckley, B. and D'Arrigo, R.D.: 1996, Interdecadal climate oscillations in the Tasmanian sector of the Southern Hemisphere: evidence from tree rings over the past three millennia. In: Jones, P. D., Bradley, R. S., Jouzel, J. (eds): *Climate variations and forcing mechanisms of the last 2,000 years*. NATO ASI Series, I41, 141–160.
- Dean, W.E.: 1997, Rates, timing, and cyclicity of Holocene eolian activity in north-central United States: evidence from varved lake sediments. *Geology*, 25, 331–334. DOI: 10.1130/0091-7613(1997)025<0331:RTACOH>2.3.CO;2
- Eddy, J.A.: 1976, The Maunder minimum. *Science, New Series*, 192, 4245, 1189–1202.
- Ekman, M.: 2003, The world's longest sea level series and a winter oscillation index for northern Europe 1774 - 2000. *Small Publications in Historical Geophysics*, 12, 31 pp.
- Fleitman, D., Burns, S.J., Mudelsee, M., Neff, U., Kramers, J., Mangini, A. and Matter, A.: 2003, Holocene forcing of the Indian monsoon recorded in a stalagmite from Southern Oman. *Science*, 300, 5626, 1737–1739.
- Haeblerli, W. and Holzhauser, H.: 2003, Alpine glacier mass changes during the past two millennia. *PAGES News*, 11, 1, 13–15.
- Hodell, D. A., Brenner, M., Curtis, J. H. and Guilderson, T.: 2001, Solar forcing of drought frequency in the Mayalaw lands. *Science*, 292, 5520, 1367–1370. DOI: 10.1126/science.1057759
- Hong, Y.T., Jiang, H.B., Liu, T.S., Zhou, L.P., Beer, J., Li, H.D., Leng, X.T., Hong, B. and Qin, X.G.: 2000, Response of climate to solar forcing recorded in a 6000-year $\delta^{18}O$ time-series of Chinese peat cellulose. *The Holocene*, 10, 1, 1–7.
- Hu, F.S., Kaufman, D., Yoneji, Su., Nelson, D., Shemesh, A., Huang, Y., Tian, J., Bond, G., Clegg, B. and Broun, T.: 2003, Cyclic variation and solar forcing of Holocene climate in the Alaskan Subarctic. *Science*, 301, 5641, 1890–1893. DOI: 10.1126/science.1088568
- Jose, P.: 1965, Sun's motion and sunspots. *Astronomical Journal*, 70, 193–200. DOI: 10.1086/109714
- Juhl, J.: 1984, The Danish Method of weight reduction for gross error detection. *XV ISP Congress Proc., Comm. III, Rio de Janeiro*.
- Kalnay, E., Kanamitsu, M., Kistler, R. et al.: 1996, The NCEP/NCAR 40-year reanalysis project. *Bulletin of the American Meteorological Society*, 77, 3, 437–471. DOI: 10.1175/1520-0477(1996)077<0437:TNYRP>2.0.CO;2
- Kegel, J.: 1987, Zur Lokalisierung grober Datenfehler mit Hilfe robuster Ausgleichungsverfahren. *Vermessungstechnik*, 35, №10, Berlin.
- Kilifarska, N.A. and Haight, J.D.: 2005, The impact of solar variability on the middle atmosphere in present day and pre-industrial atmospheres. *J. Atmos. Solar Terr. Phys.*, 67, 3, 241–249. DOI: 10.1016/j.jastp.2004.10.003

- Kilifarska, N.A., Tassev, Y.K. and Tomova, D.Y.: 2008, Cosmic ray showers and their relation to the stratospheric sudden warmings. *Sun and Geosphere*, 3, 1, 10–17.
- Kilifarska, N.A.: 2011, Long-term variations in the stratospheric winter time ozone variability – 22 year cycle. *Comptes rendus de l'Academie Bulgare des Sciences*, 64, 6, 867–874.
- Kistler, R., Collins, W., Saha S. et al.: 2001, The NCEP-NCAR 50-year reanalysis: Monthly means CD-ROM and documentation. *Bulletin of the American Meteorological Society*, 82, 2, 247–267.
DOI: 0.1175/1520-0477(2001)082<0247:TNNYRM>2.3.CO;2
- Kubik, K.: 1982, An error theory for the Danish method. *ISP Symposium, Comm. III, Helsinki*.
- Lean, J.: 2000, Evolution of the Sun's spectral irradiance since the Maunder Minimum. *Geophysical Research Letters*, 27, 16, 2425–2428.
DOI: 10.1029/2000GL000043
- Mitchell, T.D. and Jones, P.D.: 2005. An improved method of constructing a database of monthly climate observations and associated high-resolution grids. *International Journal of Climatology*, 25, 6, 693–712.
DOI: 10.1002/joc.1181
- Muscheler, R., Beer, J. and Kromer, B.: 2003, Long-term climate variations and solar effects. Processing in ISCS Symposium, Solar Variability as an Input to the Earth's Environment, SP-535. ESA, 305–316.
- Nyberg, J., Kuijpers, A., Malmgren, B.A. and Kundzendorf, H.: 2001, Late Holocene changes in precipitation and hydrography recorded in marine sediments from the northern Caribbean Sea. *Quaternary Research*, 56, 87–102. DOI: 10.1006/qres.2001.2249
- Peterson, L.C., Overpeck, J.T., Kipp, N.G. and Imbrie, I.: 1991, A high resolution Late Quaternary upwelling record from the anoxic Cariaco Basin, Venezuela. *Paleoceanography*, 6, 1, 99–119.
DOI: 10.1029/90PA02497
- Prasad, S., Vos, H., Negendank, J.F.W., Waldmann, N., Goldstein, S. and Stein, M.: 2004, Evidence from Lake Lisan of solar influence on decadal to bicentennial scale climate variability during marine oxygen isotope stage 2. *Geology*, 32, 7, 581–584.
DOI: 10.1130/G20553.1
- Qin, X., Tan, M., Liu, T., Wang, X., Li, T. and Lu, J.: 1999, Spectral analysis of a 1000-year stalagmite lamina-thickness record from Shihua Cavern, Beijing, China, and its climatic significance. *The Holocene*, 9, 6, 689–694.
- Raspopov, O.M., Dergachev, V.A. and Kolström, T.: 2004, Periodicity of climate conditions and solar variability derived from dendrochronological and other palaeoclimatic data in high latitudes. *Palaeogeography Palaeoclimatology Palaeoecology*, 209, 1, 127–139.
DOI: 10.1016/j.palaeo.2004.02.022
- Roig, F.A., Le-Quesne, C., Boninsegna, J.A., Briffa, K.R., Lara, A., Grudd, H., Jones, P.D. and Villagran, C.: 2001, Climate variability 50,000 years ago in mid-latitude Chile as reconstructed from tree rings. *Nature*, 410, 567–570. DOI: 10.1038/35069040
- Ron, C., Chapanov, Ya. and Vondrák, J.: 2012, Solar excitation of bicentennial Earth rotation oscillations. *Acta Geodyn. Geomater.*, 9, 3(167), 259–268.
- Schimmelmann, A., Lange, C.B. and Meggers, B.J.: 2003, Palaeoclimatic and archaeological evidence for a 200yr recurrence of floods and droughts linking California, Mesoamerica and South America over the past 2000 years. *The Holocene*, 13, 5, 763–778.
- Sharp, G.: 2010, Are Uranus & Neptune responsible for Solar Grand Minima and Solar Cycle Modulation? arXiv:1005.5303v3 [physics.geo-ph], 15pp.
- Solanki, S.K., Usoskin I.G., Kromer B., Schüssler, M. and Beer, J.: 2004, Unusual activity of the Sun during recent decades compared to the previous 11,000 years. *Nature*, 431, No. 7012, 1084–1087.
DOI: 10.1038/nature02995
- Sonett, C.P. and Suess, H.E.: 1984, Correlation of bristlecone pine ring widths with atmospheric carbon-14 variations: a climate-sun relation. *Nature*, 307, 5947, 141–143. DOI: 10.1038/307141a0
- Soon, W.W. and Yaskell, S.H.: 2003, The Maunder Minimum and the Variable Sun-Earth Connection. World Scientific Publishing Co. Pte. Ltd, Singapore.
- Steinhilber, F., Beer, J. and Frohlich, C.: 2009, Total solar irradiance during the Holocene. *Geophys. Res. Lett.*, 36, L19704. DOI: 10.1029/2009GL040142
- Stephenson, F.R. and Morrison, L.V.: 1984, Long-term changes in the rotation of the Earth: 700 BC to AD 1980. *Philosophical Transactions of the Royal Society of London, Ser. A*, 47–70.
- Vasilev, S.S., Dergachev, V.A. and Raspopov, O.M.: 1999, Sources of the long-term variations of the radiocarbon concentration in the Earth's atmosphere. *Geomagnetism and Aeronomy*, 39, 6, 80–89.
- Velinov, P.I.Y., Mateev L. and Kilifarska N.A.: 2005, 3-D model for cosmic ray planetary ionisation in the middle atmosphere. *Geophys.*, 23, 9, 3043–3046.
- Wagner, G., Beer, J., Masarik, J., Muscheler, R., Kubik, P.W., Mende, W., Laj, C., Raibeck, G. M. and Yiou, F.: 2001, Presence of the solar de Vries cycle about 205 years during the last ice age. *Geophysical Research Letters*, 28, 2, 303–306.
DOI: 10.1029/2000GL006116
- Wang, Y., Cheng, H., Edwards, R.L., He, Y., Kong, X., An, Z., Wu, J., Kelly, M.J., Dykoski, C.A. and Li, X.: 2005, The Holocene Asian monsoon: links to solar changes and North Atlantic climate. *Science* 308, 5723, 854–857. DOI: 10.1126/science.1106296
- Wiles, G.C., D'Arrigo, R.D., Villalba, R., Calkin, P.E. and Barclay, D.J.: 2004, Century-scale solar variability and Alaskan temperature change over past millennium. *Geophysical Research Letters* 31, L15203. DOI: 10.1029/2004GL020050
- Yang, B., Braeuning, A., Johnson, K.R. and Yafeng, S.: 2002, General characteristics of temperature variation in China during the last two millennia. *Geophysical Research Letters*, 29, 9, 1324.
DOI: 10.1029/2001GL014485
- Zolitschka, B.: 1996, High resolution lacustrine sediments and their potential for palaeoclimatic reconstruction. In: Jones, P.D., Bradley, R.S., Jouzel, J. (Eds.), *Climate Variations and Forcing Mechanism of the Last 2000 years*. NATO ASI Series, 141. Springer-Verlag Berlin, Heidelberg, 454–478.